Effects of Water Vapor on Gas Permeation and Separation Properties of MFI Zeolite Membranes at High Temperatures

Haibing Wang and Y. S. Lin
Chemical Engineering, School for Engineering of Matter, Transport and Energy, Arizona State University, Tempe, AZ 85287

DOI 10.1002/aic.12622
Published online April 27, 2011 in Wiley Online Library (wileyonlinelibrary.com).

Understanding the effects of water vapor on gas permeation and separation properties of MFI zeolite membranes, especially at high temperatures, is important to the applications of these zeolite membranes for chemical reactions and separation involving water vapor. The effects of water vapor on H_2 and CO_2 permeation and separation properties of ZSM-5 (Si/Al ~ 80) zeolite and aluminum-free silicalite membranes were studied by comparing permeation properties of H_2 and CO_2 with the feed of equimolar H_2/CO_2 binary and $H_2/CO_2/H_2O$ ternary mixtures in 300–550°C. For both membranes, the presence of water vapor lowers H_2 and CO_2 permeance to the same extent, resulting in negligible effect on the H_2/CO_2 separation factor. The suppression effect of water vapor on H_2 and CO_2 permeation is larger for the less hydrophobic ZSM-5 zeolite membrane than for the hydrophobic silicalite membrane, and, for both membranes, is stronger at lower temperatures and higher water vapor partial pressures. © 2011 American Institute of Chemical Engineers *AIChE J,* 58: 153–162, 2012
Keywords: MFI zeolite membranes, suppression effect, water vapor adsorption, $H_2/CO_2/H_2O$ ternary system

Introduction

MFI-type zeolites are crystalline aluminosilicates with molecular-scale pores constructed by the 10-membered oxygen rings. Because of the small pore openings and uniform pore size distribution in the crystal structure, MFI zeolite membranes can be used to separate small gas mixtures and organic isomers by gas/vapor permeation[1–3] and azeotropic, close-boiling, and heat sensitive organic mixtures through pervaporation.[4–6] Gas or liquid mixtures whose components have different adsorption affinities with zeolitic pores can also be separated by MFI zeolite membranes, as the component with strong adsorption on zeolitic pores blocks the zeolitic pore channels for the permeation of the weakly adsorbing component through the membrane, resulting in a high selectivity for the strongly adsorbing component over the weakly adsorbing component.[7]

The suppression effect of a strongly adsorbing component on the permeation of a weakly adsorbing component through MFI zeolite membranes was observed in many binary gas systems. The permeation of H_2 was strongly suppressed by the adsorbing components, such as n-C_4H_{10} and CO_2, at low temperatures.[8] As temperature increases, the permeance of n-C_4H_{10} decreases, whereas the H_2 permeance increases due to the weakening of the adsorption between n-C_4H_{10} and MFI zeolitic pores. Because of the suppression effect of CO_2 on H_2 permeation through the MFI zeolite membranes at low temperatures, the quality of MFI zeolite membranes can be evaluated by measuring the H_2/CO_2 separation factor of the membranes at room temperature.[9] High quality membranes

Correspondence concerning this article should be addressed to Y. S. Lin at jerry.lin@asu.edu.

with few defects show high CO_2/H_2 separation factor at room temperature due to the adsorption of CO_2 molecules into zeolitic pores and suppression of H_2 permeation through the membrane by blocking the zeolitic pores. Similarly, CO_2/N_2 separation factor of 13.7 on a Na-ZSM zeolite membrane was reported because the preferential adsorption of CO_2 molecules into zeolitic pores hindered the permeation of N_2 through the membrane.[10]

MFI zeolite membranes also offer applications in separation of organics/water mixtures by pervaporation because organics and water have different adsorption affinities with zeolitic pores.[11] High silica hydrophobic MFI zeolite (silicalite) membranes are used for removal of organics from water, whereas the hydrophilic MFI zeolite (ZSM-5) membranes are used to remove water from organics (dehydration),[12] because the hydrophobic and hydrophilic zeolite membranes adsorb preferentially organics and water respectively. The hydrophobicity/hydrophilicity of MFI zeolite membranes is affected significantly by the aluminum content in the zeolite framework. As the aluminum content in the zeolite framework increases, the saturation loading of water in the zeolites increases.[13] Despite of the hydrophobic nature of pure silicalite, water vapor adsorption with a low saturation loading in zeolitic pores of silicalites was also observed.[13,14]

Noack et al.[15] measured the water vapor permeation fluxes through MFI zeolite membranes with different Si/Al ratios at low temperatures (105°C). It was found that H_2O/H_2 permselectivity for the ZSM-5 membrane was much higher than that for the silicalite membrane due to the strong adsorption capability of the ZSM-5 membrane for water vapor. Zhu et al.[16] studied water vapor permeation by a zeolite-4A membrane from 30°C to 100°C. Although the water vapor partial pressures in the H_2O/CO, H_2O/H_2, and H_2O/CH_4 binary systems were very low (2.24 kPa for water vapor compared with the 101.3 kPa for the total pressure), water vapor had a strong suppression effect on the permeation of the other component in these binary systems. The water vapor permeance was two orders of magnitude higher than that of the other component in these binary systems. The suppression effect was ascribed to the strong adsorption affinity of H_2O inside the zeolite-4 Å pores, which blocked the permeation of the second gas component through the membrane.

Gas permeation through MFI zeolite membranes in the presence of water vapor at high temperatures (above 300°C) is technically important to the applications of MFI zeolite membranes for chemical reactions and separation involving water vapor, such as water gas shift reaction for hydrogen production.[17] The water gas shift reaction was operated in the modified MFI zeolite membrane reactor with improved H_2/CO_2 separation performance in 400–550°C with H_2O/CO ratios between 1.0 and 3.5.[17] A study on the permeation of H_2 and CO_2 through MFI zeolite membranes at high temperatures in the presence of water vapor is needed to understand the effects of water vapor on the permeation of H_2, CO_2 through the MFI membrane reactor. Although MFI membranes without post-synthetic modification for separation performance improvement were used in this study, the results are still very helpful to elucidate the effects of water vapor on the permeation of H_2 and CO_2 through the modified MFI zeolite membrane reactor used for water gas shift reaction. The objective of this work is to study the effects of water vapor on H_2/CO_2 permeation and separation properties of MFI zeolite membranes with different degree of hydrophobicity at high temperatures. A silicalite (MFI zeolite with Si/Al $= \infty$) and a ZSM-5 (MFI zeolite with Si/Al $\sim$ 80) membrane was, respectively, prepared on alumina support coated with yttria stabilized zirconia (YSZ) as the barrier layer to prevent transport of aluminum from the support to the zeolite layer, and used to study the effects of water vapor on gas permeation and separation properties of the membranes.

Experimental

Support preparation and zeolite membrane synthesis

Macroporous α-alumina supports with a porosity of around 45% and an average pore size of around 0.2 μm were prepared by pressing the α-alumina powder (Alcoa, A-16) and sintering at high temperatures. The sintered α-alumina porous supports were polished with SiC polishing papers until the surface was shiny. It is known that it was difficult to prepare pure silica silicalite membrane on alumina support due to transfer of aluminum from the support via directly solid state diffusion and indirectly dissolution into the synthesis solution.[18] To prevent transport of aluminum from the support via solid state diffusion, an yttria stabilized zirconia (YSZ) layer was dip-coated onto the surface of the polished α-alumina porous supports as a barrier layer.

The YSZ suspension for the dip-coating was prepared according to the procedure reported by our group in the previous publication.[18] The YSZ suspension coated α-alumina porous supports were dried in an oven at 40°C for 2 days, followed by sintering at 1000°C in air for 3 h. The heating and cooling rates of the sintering process were 100°C/h. The dip-coating and sintering of the YSZ suspension coated alumina supports were repeated thrice to obtain a suitable thickness of the YSZ barrier layer and ensure the adequate coverage of the supports with YSZ suspension.

Aluminum-free silicalite and ZSM-5 membranes with YSZ barrier layer were prepared by the secondary growth method. The macroporous α-alumina porous supports with YSZ barrier layer were coated with silicalite seed layer using silicalite suspension described in the previous publications.[19,20] Briefly, a solution was first prepared by dissolving fumed silica (Sigma-Aldrich, particle size: 0.007 μm, surface area: 390 ± 40 m^2/g) and sodium hydroxide (NaOH, EMD Chemicals) into the tetrapropylammonium hydroxide (TPAOH, 1 M in water, Sigma-Aldrich) solution at 80°C under magnetic stirring. The final molar composition of the solution was 10 SiO_2: 2.4 TPAOH: 1 NaOH: 110 H_2O. The solution was hydrothermally treated at 125°C for 8 h to obtain the MFI zeolite suspension. The YSZ coated α-alumina porous supports were then dip-coated with 2 wt % silicalite suspension, followed by drying and calcination at 550°C in air for 8 h. The dip-coating of silicalite suspension and calcination of the seeded supports were repeated thrice.

The solution for the secondary growth of MFI zeolite membranes was prepared according to the procedure reported by Xomeritakis et al.[21] The solution was prepared by dissolving KOH pellets (Sigma-Aldrich), tetrapropylammonium bromide (TPABr, Sigma-Aldrich) into deionized

Table 1. Major Characteristics of Silicalite and ZSM-5 Membranes Prepared in This Work

Membrane	Silicalite	ZSM-5
Secondary growth solution	1 KOH: 1 TPABr: 4.5 SiO_2: 18 C_2H_5OH: 1000 H_2O	1.5 KOH: 1 TPABr: 4.5 SiO_2: 18 C_2H_5OH: 1000 H_2O: 0.028 $Al_2(SO_4)_3 \cdot 18H_2O$
Si/Al ratio in secondary growth solution	∞	80
KOH concentration in secondary growth solution	0.056 mol/L	0.084 mol/L
Si/Al ratio in final membrane	∞	79
Membrane thickness	21 μm	12.5 μm
The Helium permeance before template removal at room temperature	1.18×10^{-9} mol m^{-2} s^{-1} Pa^{-1}	1.49×10^{-9} mol m^{-2} s^{-1} Pa^{-1}

water under magnetic stirring. The solution was heated to 80°C, and then tetraethylorthosilicate (TEOS, 98% Sigma-Aldrich) was added dropwise into the above solution for hydrolysis. The mixture solution was stirred at 80°C until a clear solution was obtained. For the synthesis of ZSM-5 membrane, some aluminum sulfate ($Al_2(SO_4)_3 \cdot 18H_2O$, Sigma-Aldrich) was added into the above solution as the aluminum source. The molar composition of the final solution was 1 KOH: 1 TPABr: 4.5 SiO_2: 18 C_2H_5OH: 1000 H_2O for preparing the silicalite membranes, and 1.5 KOH: 1 TPABr: 4.5 SiO_2: 18 C_2H_5OH: 1000 H_2O: 0.028 $Al_2(SO_4)_3 \cdot 18H_2O$ for preparing the ZSM-5 membranes. More KOH was added into the solution for synthesis of ZSM-5 membranes than silicalite membranes in order to allow incorporation of the aluminum source from solution into the zeolite framework.

The synthesis solution was cooled down to room temperature and aged for about 4 h. After that, the clear solution was filtered and transferred into a Teflon-lined stainless steel autoclave in which several MFI zeolite seeded porous supports were put vertically at the bottom. Hydrothermal synthesis of zeolite membranes was conducted at 175°C for 8 h. The synthesized membranes were washed with deionized water for several times, then dried, and calcined at 550°C for 8 h in air to remove the template. Synthesis conditions and major characteristics of the silicalite and ZSM-5 membranes prepared in this work are summarized in Table 1.

Membrane characterization and gas permeation/separation experiments

After the template was removed, the crystal structure of the synthesized MFI zeolite membranes was characterized by X-ray diffraction (XRD) (Bruker AXS-D8, Cu Kα radiation) with 2θ from 5° to 45° at a step size of 0.015°. The morphology and thickness of the MFI zeolite membranes were characterized using a scanning electron microscopy (SEM, Philips, XL 30). The composition of the MFI zeolite membranes synthesized from solutions with different aluminum contents were analyzed by energy dispersive X-ray spectroscopy (EDS).

Figure 1 shows a schematic illustration of the setup for H_2/CO_2 binary and $H_2/CO_2/H_2O$ ternary gas permeation/separation experiments. Before water vapor was introduced into the permeation cell, the H_2, CO_2 permeance and H_2/CO_2 separation factor for the H_2/CO_2 binary gas permeation through the MFI zeolite membrane were measured from 300°C to 550°C. During the binary gas permeation experiments, an equimolar H_2/CO_2 mixture gas was fed into the feed side of the permeation cell. The gas composition on the permeate side was continuously analyzed by a gas chromatograph (GC, Agilent, 6890N) equipped with a thermal conductivity detector (TCD) and a Hayesep® DB packed column (Alltech).

After that, water was introduced by a precisely calibrated liquid pump (LC-20AD, Shimadzu Corporation) and was

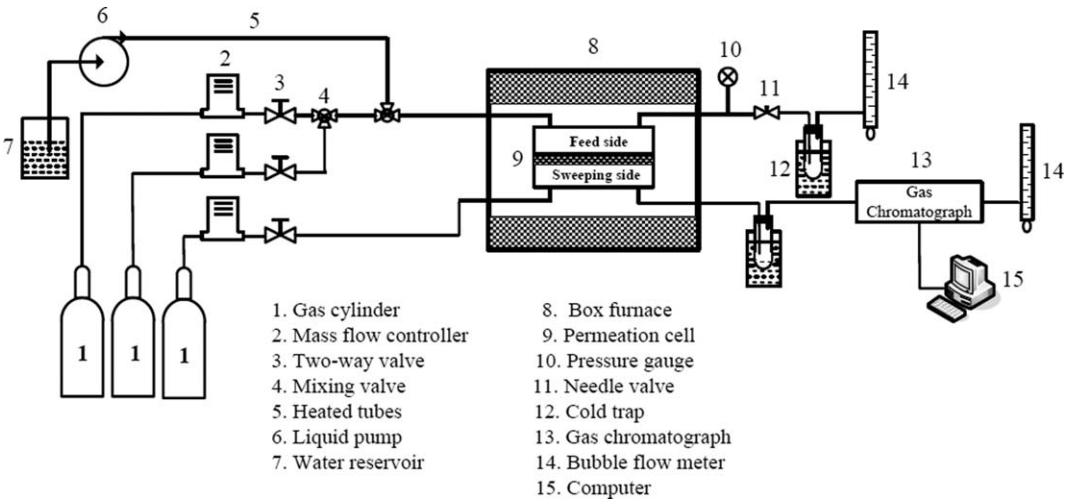

Figure 1. A schematic illustration of the set up for the gas permeation experiments in the presence of water vapor.

carried into the permeation cell using an equimolar H_2/CO_2 mixture gas ($P_{H_2} = P_{CO_2} = 76$ kPa in the permeation cell). The flow rate of water was precisely controlled so that the $H_2/CO_2/H_2O$ ternary gas mixture in the permeation cell was equimolar ($P_{H_2} = P_{CO_2} = P_{H_2O} = 76$ kPa in the permeation cell) and the total pressure for the equimolar H_2, CO_2 and H_2O mixture gas in feed side of the permeation cell was 228 kPa. The water vapor permeance was measured from 300°C to 550°C by a weighing method reported by Tsuru et al.[22] Water vapor on rententate and permeate sides was condensed with cold traps (in ice-water mixture), and its permeance was calculated based on the weight of water collected on permeate side in a period of time and the transmembrane partial pressure of water vapor. The flow rates and compositions of the noncondensable gases, such as H_2 and CO_2 in $H_2/CO_2/H_2O$ ternary system, were measured by bubble flow meters and GC to calculate H_2 and CO_2 permeances, and H_2/CO_2 separation factor. The H_2 and CO_2 permeances as well as the H_2/CO_2 separation factor for the $H_2/CO_2/H_2O$ ternary gas mixture were compared with those for the H_2/CO_2 binary gas mixture to study the effect of water vapor on the permeation of H_2 and CO_2 through MFI zeolite membranes.

The effect of water vapor partial pressure on the permeation of H_2 and CO_2 through the MFI zeolite membranes was studied by measuring the component permeance as a function of water vapor partial pressure in $H_2/CO_2/H_2O$ ternary system at different temperatures. In these experiments, the partial pressures of H_2 and CO_2 were kept constant and equimolar ($P_{H_2} = P_{CO_2} = 76$ kPa), whereas the partial pressure of water vapor in $H_2/CO_2/H_2O$ ternary system increased to 236 kPa by increasing the water flow rate. The total gas pressure in the feed side of the permeation cell increased from 152 to 388 kPa as more and more water vapor was fed into the permeation cell. $H_2/CO_2/H_2O$ ternary gas permeation through both silicalite and ZSM-5 zeolite membranes was conducted, and the results were compared as MFI zeolite membranes with different Al contents in the framework have different water vapor adsorption capacities that in turn have different suppression effect on H_2 and CO_2 permeation through the zeolite membranes.

Results and Discussion

Characteristics of silicalite and ZSM-5 membranes

The characteristics of the two MFI zeolite membranes with different Si/Al ratio by SEM, XRD, and EDS are given in Figures 2–5. Figure 2 shows the SEM image of the membrane surface and the XRD spectrum of the silicalite membrane synthesized at 175°C for 8 h. As can be seen from this figure, a crack-free continuous zeolite membrane with good intergrowth between zeolite crystals was obtained. XRD spectrum shows that some sort of orientation in zeolite crystals was developed for this membrane. It was reported that MFI zeolite membranes with different orientations could be obtained by only varying the synthesis time and hydrothermal synthesis temperature.[23] The orientation developed in the silicalite membranes is due to the competitive growth of zeolite crystals during the secondary growth process. Randomly oriented MFI zeolite membrane was obtained from an aluminum-free synthesis solution after being synthesized for 4 h by the secondary growth method, as the synthesis time was not long enough for zeolite crystals to orient themselves.[23] However, as the synthesis time increased to 8 h, orientation in zeolite crystals started to occur as observed in this study.

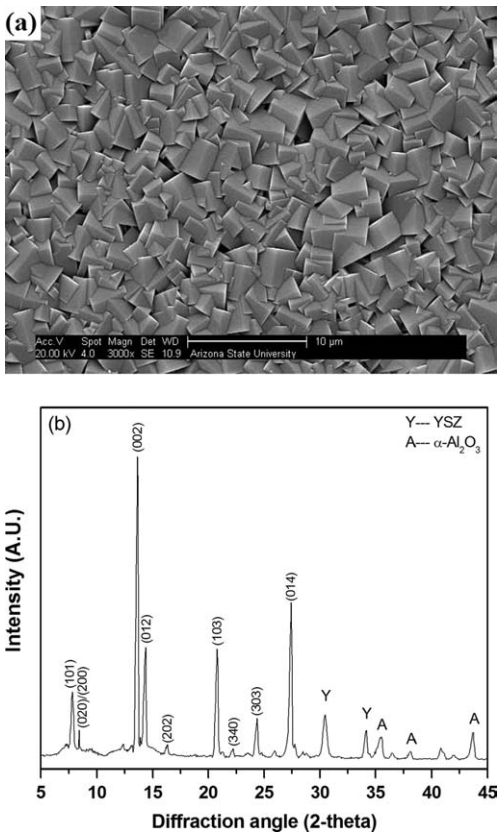

Figure 2. (a) SEM micrograph of the silicalite membrane surface and (b) XRD spectrum of the silicalite membrane grown on an YSZ coated α-alumina porous support.

Figure 3 shows cross-sectional view of the silicalite membranes and results of EDS analysis on silicalite layer. As shown, the thickness of the silicalite layer is about 21 μm. The EDS result shows that the silicaltie membrane contains no aluminum. It is known that aluminum might transport from the α-alumina porous supports into zeolite layer during the hydrothermal synthesis process and high temperature calcination for the template removal.[19,20] In this work, aluminum transport from α-alumina porous supports into zeolite membranes during the calcination process and the dissolution of α-alumina porous supports during the hydrothermal synthesis process were effectively avoided by the following two approaches. First, an YSZ barrier layer was coated onto the surface of the α-alumina porous support in this study. This YSZ layer served as the barrier layer that prevented solid state transport of aluminum from the support to the silicalite layer during calcination. The second approach was to reduce the dissolution of aluminum from the support into the synthesis solution by lowering the pH of the synthesis solution used in the secondary growth step (pH $\sim$ 14).[24] In this work, pH of the synthesis was maintained at about 11.5 as measured by pH papers to minimize dissolution of aluminum into the synthesis solution.

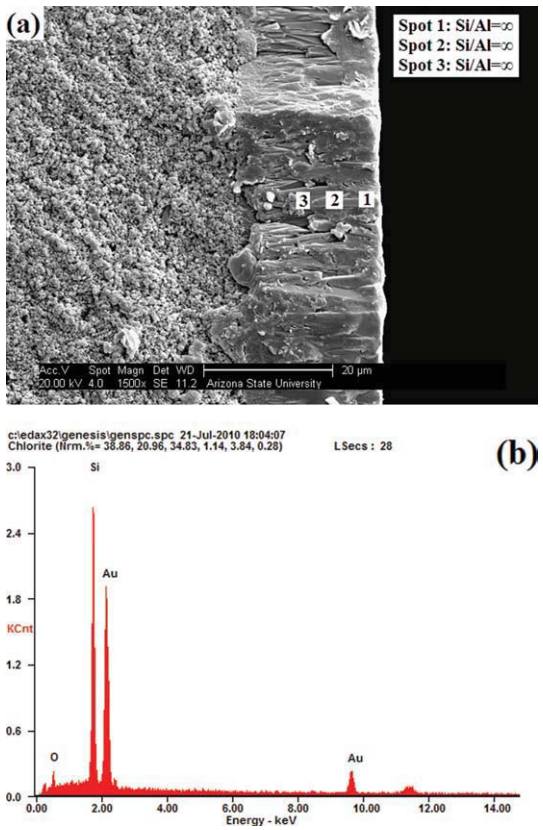

Figure 3. (a) EDS elemental analysis on the cross section of the silicalite membrane grown on an YSZ coated α-alumina porous support and (b) EDS spectrum of the analysis on the cross section of the silicalite membrane.

[Color figure can be viewed in the online issue, which is available at wileyonlinelibrary.com.]

SEM micrograph and XRD pattern of the ZSM-5 membrane synthesized from a solution with Si/Al = 80 are shown in Figure 4. Similar to the silicalite membrane, zeolite crystals of the ZSM-5 membrane are intergrown with each. The membrane was randomly oriented as verified by the XRD and has a thickness of only 12.5 μm. These are different from the silicalite membrane, indicating that aluminum source in the synthesis solution affected the competitive growth and orientation development of zeolite membranes. Uguina et al.[25] studied the effect of SiO_2/Al_2O_3 molar ratio on the crystallization kinetics of ZSM-5 membranes and found that high aluminum content in the gel led to the longer induction time and inhibited the formation of ZSM-5 zeolite crystals at the beginning of the crystallization. The thinner ZSM-5 membrane compared to the silicalite membrane is probably due to the retardation effect of aluminum in the synthesis solution on the crystal growth. Figure 5 shows the Si/Al ratio along the cross section of the ZSM-5 membrane. The EDS measurement results showed that Si/Al ratio in the zeolite membrane is similar to that in the synthesis solution, confirming that almost no aluminum was dissolved from the support and subsequently incorporated into the zeolite membrane during the hydrothermal synthesis process. Although more KOH was added into the solution for ZSM-5 membrane synthesis, the pH of the solution was not high enough to cause leaching of aluminum from the macroporous α-alumina support during the hydrothermal synthesis of the membrane.

H_2 and CO_2 permeation/separation properties of silicalite and ZSM-5 zeolite membranes

Figures 6 and 7 show the gas/vapor permeation with equimolar H_2/CO_2 binary and $H_2/CO_2/H_2O$ ternary mixture feed through the silicalite and ZSM-5 membrane as a function of temperature in 300–550°C. H_2 and CO_2 permeances in H_2/CO_2 binary mixture are similar for both membranes, and decrease as temperature increases. The H_2 and CO_2 permeances are approximately proportional to $T^{-1/2}$. In this temperature range, the temperature dependence of H_2 and CO_2 permeances in H_2/CO_2 binary system is similar to their single gas permeation properties at high temperatures due to the negligible adsorption of H_2 and CO_2 on MFI zeolites at high temperatures. The results are consistent with earlier results that gas permeance of H_2, CO and CO_2 with single component feed is similar to that with the $H_2/CO_2/CO$ ternary feed at temperatures above 300°C reported by Kanezashi and Lin.[26]

H_2, CO_2, and H_2O permeances with equimolar $H_2/CO_2/H_2O$ ternary mixture feed for the silicalite and ZSM-5 membranes as a function of temperature are also shown in

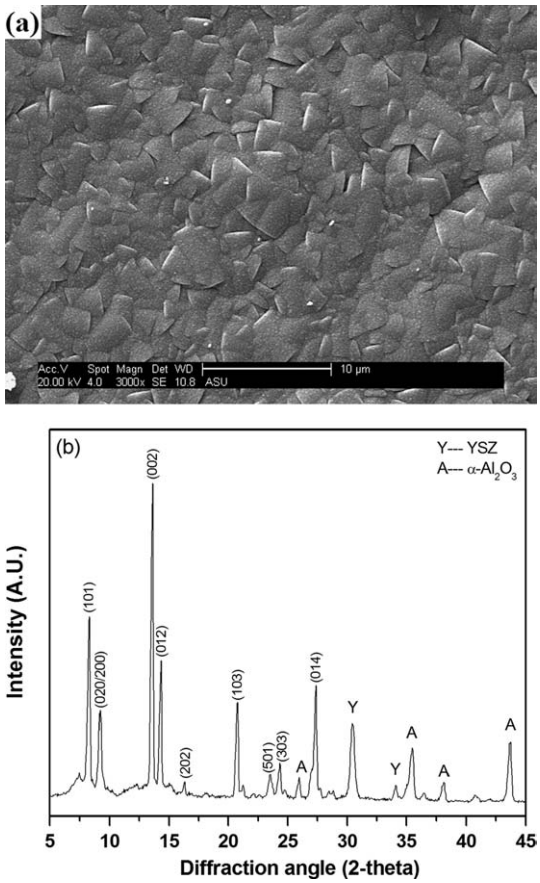

Figure 4. (a) SEM micrograph of the ZSM-5 zeolite membrane surface and (b) XRD spectrum of the ZSM-5 zeolite membrane grown on an YSZ coated α-alumina porous support.

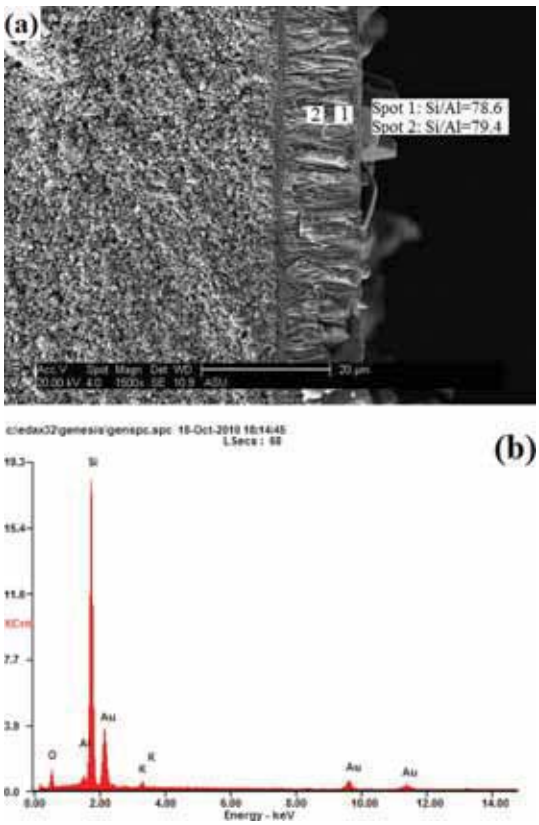

Figure 5. (a) EDS elemental analysis on the cross section of the ZSM-5 zeolite membrane grown on an YSZ coated α-alumina porous support and (b) EDS spectrum of the analysis on the cross section of the ZSM-5 zeolite membrane.

[Color figure can be viewed in the online issue, which is available at wileyonlinelibrary.com.]

Figures 6 and 7. Both H_2 and CO_2 permeances with $H_2/CO_2/H_2O$ ternary mixture feed are lower than those in H_2/CO_2 binary system, indicating that water vapor has a suppression effect on H_2 and CO_2 permeation through the silicalite and ZSM-5 zeolite membranes. There is more reduction in H_2 and CO_2 permeances caused by water vapor for ZSM-5 zeolite membrane than the silicalite membrane. At 550°C, the water vapor permeance is 103 and 12 times lower than hydrogen permeance for the silicalite and ZSM-5 membranes. Clearly, water vapor has higher permeance and more effects on reducing H_2 and CO_2 permeance for ZMS-5 zeolite membrane than silicalite membrane because the former containing some Al in the zeolite framework is more hydrophilic than the latter. However, the observation of water vapor permeation through the silicalite membrane indicates that the synthesized silicalite membrane is not entirely hydrophobic as was expected from the absence of Al in the zeolite framework.

Several studies also showed suppression effect of water vapor on gas permeation in MFI zeoltie membranes at low temperatures (<300°C).[15,27] The suppression effect of an adsorbing component on the permeation of a nonadsorbing component is well known for zeolite membranes.[28,29] However, the results obtained in this study show for the first time appreciable adsorption of water vapor on silicaltie and ZMS-5 zeolites at high temperatures in 300–500°C, and the suppression effect of water vapor on the gas permeation through silicalite and ZSM-5 zeolite membranes in this temperature range. It is found that water vapor exhibits negligible effects on gas permeance through silicalite membranes at even higher temperature (>550°C).

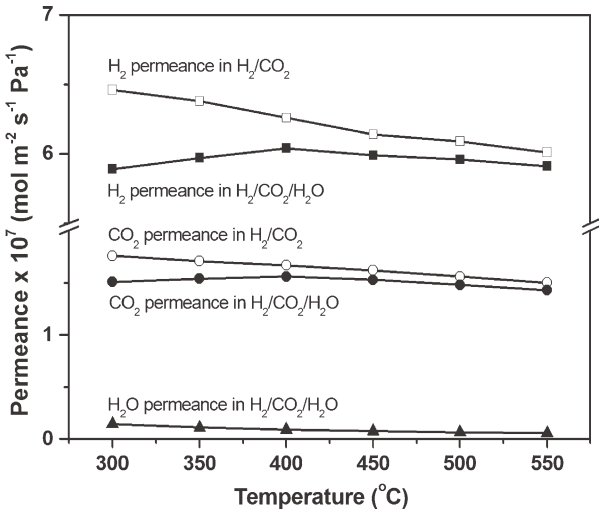

Figure 6. Gas permeation through the silicalite membrane with equimolar H_2/CO_2 binary mixture (open symbols, $P_{H_2} = P_{CO_2} = 76$ kPa) and equimolar $H_2/CO_2/H_2O$ ternary mixture (closed symbols, $P_{H_2} = P_{CO_2} = P_{H_2O} = 76$ kPa) as feed.

The hydrophilicity of MFI zeolites depends on the number of Lewis *cus* framework Al(III) acidic sites, Brønsted $Si(OH)^+Al^-$ acidic sites and Si—OH groups.[30,31] The Lewis *cus* framework Al(III) acidic sites and Brønsted $Si(OH)^+Al^-$

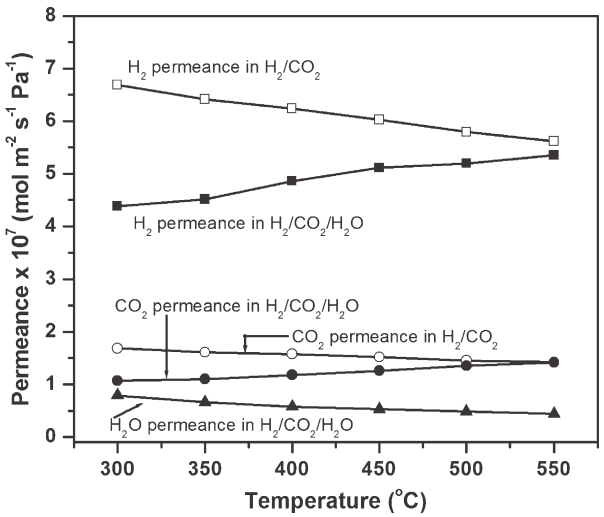

Figure 7. Gas permeation through the ZSM-5 membrane with equimolar H_2/CO_2 binary mixture (open symbols, $P_{H_2} = P_{CO_2} = 76$ kPa) and equimolar $H_2/CO_2/H_2O$ ternary mixture (closed symbols, $P_{H_2} = P_{CO_2} = P_{H_2O} = 76$ kPa) as feed.

acidic sites are formed due to the incorporation of aluminum source into the zeolite framework, whereas the Si—OH groups, a kind of typical point defects in MFI zeolites are formed to compensate Si vacancies in MFI zeolite framework. It was reported that the Si—OH groups in silicalite zeolite framework can be very high[32] and the presence of Si—OH groups and Si—OH groups boned to adsorbed water, Si—OH—$(H_2O)_n$ in silicalite membranes was confirmed by proton MAS NMR spectra of silicalite.[31] Membrane synthesis method has strong effect on the number of Si—OH groups in silicalites. Generally, more Si—OH groups are formed in the silicalite samples synthesized from an alkaline solution, whereas almost no Si—OH groups are formed in silicalites synthesized in a fluoride medium.[31] Because of the presence of Si—OH groups in the defective silicalites, adsorption of water vapor on silicalite was observed.[30] The population of Si—OH groups in the zeolite framework has significant effect on the water adsorption capacity of silicalite zeolites. Although the number of Si—OH groups in MFI zeolite decreases as the heat treatment temperature increases,[13] Si—OH groups may exist in MFI zeolites heat-treated at temperatures up to 600–800°C.[13,33]

The temperature dependence of the H_2/CO_2 separation factor with H_2/CO_2 binary mixture and $H_2/CO_2/H_2O$ ternary mixture feed is shown in Figure 8. The H_2/CO_2 separation factor for the mixture with and without water vapor is essentially the same for both membranes. This indicates that the presence of water vapor suppresses gas permeation for H_2 and CO_2 to the same extent. The results suggest that at high temperatures water vapor has same effects on lowering the permeation rate of other gas, regardless of gas type and zeolite surface-gas molecule interactions. Coudert et al.[34] studied the water-water and water-zeolite interactions for water molecules confined in zeolite nanopores using the Monte-Carlo and first-principles Car-Parrinello molecular dynamics simulations. The results showed that water confined in the hydrophobic zeolites behaves as a nanodroplet with hydrogen bonds closed to itself and some short-lived dangling OH groups, whereas water confined in the hydrophilic zeolites opens up to form weak hydrogen bonds with oxygen atoms of the zeolite framework. Although this simulation is done on LTA zeolites, the findings may also explain our experimental results. The formation of water nanodroplets in hydrophobic zeolites and hydrogen bonds between water molecules and oxygen atoms of the zeolite framework in hydrophilic zeolites indicates that as long as water molecules are adsorbed into MFI zeolitic pores with pore size of around 0.56 nm, both H_2 and CO_2 molecules are not able to surpass water molecules confined in the MFI zeolitic pores. As a result, water vapor has same suppression effect on H_2 and CO_2 permeation through the MFI zeolite membranes regardless whether they are hydrophobic or hydrophilic. Because of the lower diffusivity of water confined in MFI zeolitic pores than H_2 and CO_2, water vapor shows suppression effect on H_2 and CO_2 permeation through the MFI zeolite membranes.

Figures 9a–c show the effect of water vapor partial pressure on H_2 and CO_2 permeation through the silicalite membrane at different temperatures. At a fixed temperature, both H_2 and CO_2 permeances decrease as water vapor partial pressure in $H_2/CO_2/H_2O$ ternary system increases. As water

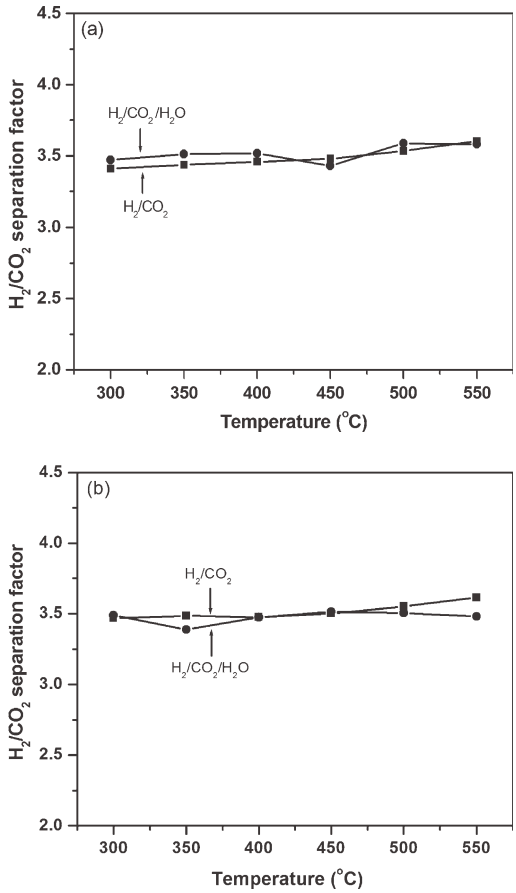

Figure 8. H_2/CO_2 separation factor with equimolar H_2/CO_2 binary mixture (square) and $H_2/CO_2/H_2O$ ternary mixture (circle) as feed for silicalite (a) and ZSM-5 zeolite (b) membranes.

vapor permeation flux through the silicalite membrane increases with its partial pressure in the ternary system, more H_2O adsorbs into zeolitic pores at a higher water vapor partial pressure. Hence, more zeolitic pores are blocked by water vapor molecules at a higher water vapor partial pressure, resulting in the decrease of H_2 and CO_2 permeances. As shown in this figure, the suppression effect of water vapor on H_2 and CO_2 permeation is stronger at a lower temperature, indicating that the preferential adsorption of water vapor into the zeolitic pores is stronger at low temperatures. Figure 9 also shows that the H_2/CO_2 separation factor for the permeation of the $H_2/CO_2/H_2O$ ternary gas through the silicalite membrane is independent of the water vapor partial pressure at a fixed temperature and is similar to the H_2/CO_2 separation factor for the permeation of the H_2/CO_2 binary gas in the absence of water vapor. As discussed above, water confined in MFI zeolitic pores has same suppression effect on the permeation of H_2 and CO_2 due to the formation of either nonadroplets or hydrogen bonds between water molecules and oxygen atoms of zeolite framework, resulting in the same H_2/CO_2 separation factor for the permeation of H_2/CO_2 binary and $H_2/CO_2/H_2O$ ternary mixture gas.

Figure 10 shows the effect of water vapor partial pressure on H_2 and CO_2 permeation through the ZSM-5 zeolite membrane at different temperatures. The water vapor has a

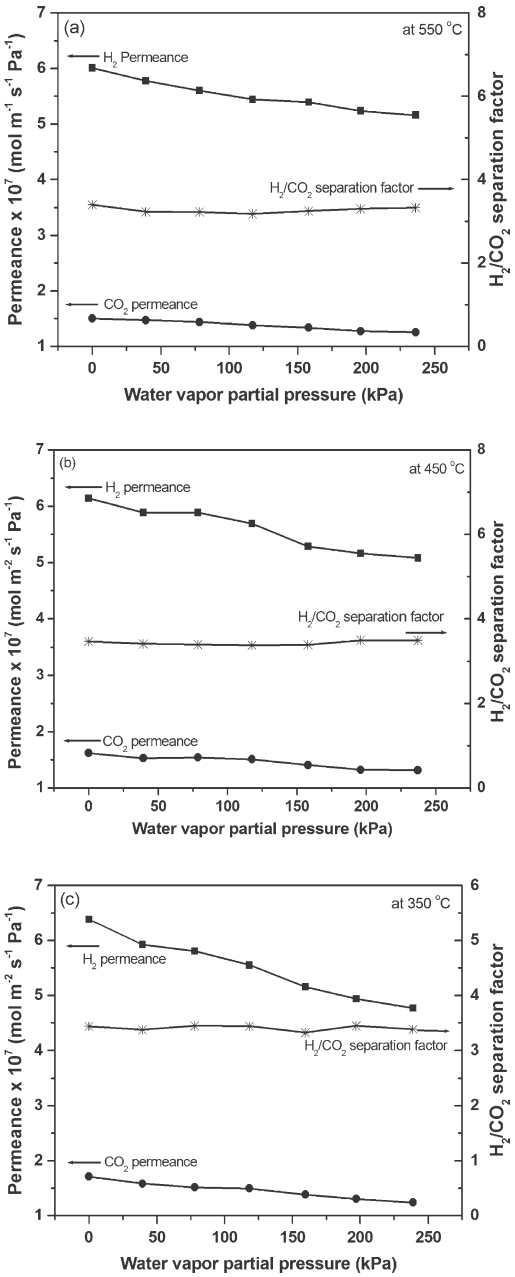

Figure 9. Effect of water vapor partial pressure on H_2 and CO_2 permeation through the silicalite membrane at different temperatures: (a) at 550°C, (b) at 450°C, and (c) at 350°C, (P_{H_2} = P_{CO_2} = 76 kPa).

stronger suppression effect on H_2 and CO_2 permeation through the ZSM-5 membrane at a lower temperature and a higher water vapor partial pressure in the $H_2/CO_2/H_2O$ ternary system, which is similar to the results observed on the silicalite membrane. Because of the stronger adsorption between water vapor and ZSM-5 zeolitic pores, the suppression effect of water vapor on H_2 and CO_2 permeation through the ZSM-5 membrane is much stronger than that through the silicalite membrane. For example, at 550°C, when the water vapor partial pressure in $H_2/CO_2/H_2O$ ternary system is 37.5 kPa, the H_2 and CO_2 permeances through the ZSM-5 membrane are 5.52×10^{-7} mol m^{-2} s^{-1} Pa^{-1} and 1.42×10^{-7} mol m^{-2} s^{-1} Pa^{-1}, respectively. As the water vapor partial pressure in the ternary system increases to 237.6 kPa, the H_2 and CO_2 permeances decreases to 3.49×10^{-7} mol m^{-2} s^{-1} Pa^{-1} and 0.94×10^{-7} mol m^{-2} s^{-1} Pa^{-1}, respectively (Figure 10a). However, for the silicalite membrane, as the water vapor partial pressure increases from 38.9 to 236 kPa at 550°C, the H_2 permeance decreases from 5.78×10^{-7} mol m^{-2} s^{-1} Pa^{-1} to 5.16×10^{-7} mol m^{-2} s^{-1} Pa^{-1}, whereas the CO_2 permeance decreased from 1.47×10^{-7} mol m^{-2} s^{-1} Pa^{-1} to 1.25 ×

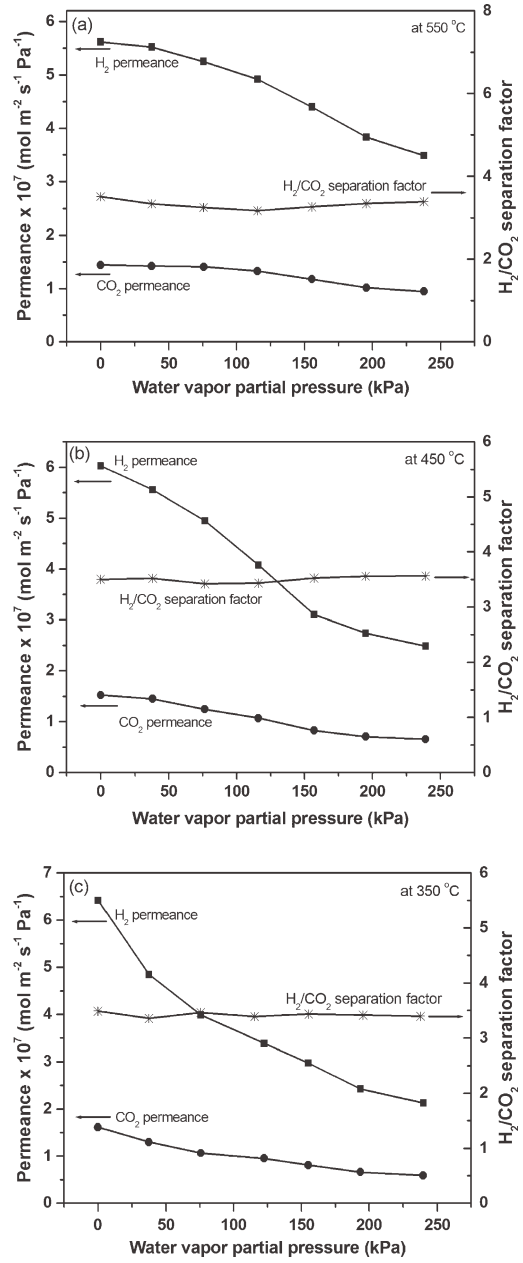

Figure 10. Effect of water vapor partial pressure on H_2 and CO_2 permeation through the ZSM-5 zeolite membrane at different temperatures: (a) at 550°C, (b) at 450°C, and (c) at 350°C, (P_{H_2} = P_{CO_2} = 76 kPa).

10^{-7} mol m^{-2} s^{-1} Pa^{-1} (Figure 9a). As the temperature decreases from 550°C to 350°C, the suppression of water vapor on the H_2 and CO_2 permeation through the ZSM-5 membrane becomes more significant due to the stronger adsorption affinity between water vapor and zeolitic pores at lower temperatures.

As also shown in Figure 10, the H_2/CO_2 separation factor for the $H_2/CO_2/H_2O$ ternary gas permeation through the ZSM-5 zeolite membrane is independent of the water vapor partial pressure, similar to the observation on the silicalite membrane shown in Figure 9. These results further confirm that the water confined in MFI zeolitic pores has same suppression effect on the permeation of H_2 and CO_2 through the MFI zeolite membrane as observed on silicalite membrane.

Conclusions

MFI zeolite membranes with controlled Si/Al ratio (aluminum-free silicalite and ZSM-5 zeolite with Si/Al ratio of about 80) can be prepared on alumina support coated with yttria stabilized zirconia barrier layer using synthesis solution of low pH and controlled aluminum content. The effects of water vapor on the permeation of H_2 and CO_2 through the two MFI zeolite membranes of the different Si/Al ratio was studied by measuring the permeance of H_2 and CO_2 with the feed of equimolar H_2/CO_2 binary and $H_2/CO_2/H_2O$ ternary mixture at different temperatures. The suppression effects of water vapor on H_2 and CO_2 permeation through MFI zeolite membranes increase as temperature decreases and water vapor partial pressure increases, and are larger for the MFI zeolite membrane with Si/Al ratio of 80 (ZSM-5 zeolite membrane) than for the aluminum-free MFI zeolite (silicalite) membrane. However, the presence of water vapor does not affect the H_2/CO_2 separation factor for both membranes. The results show that both ZSM-5 and silicalite membranes adsorb water vapor even at temperatures in the range of 300–550°C, reducing the permeability of H_2 and CO_2 in the zeolitic pores of these membranes.

Acknowledgments

The authors thank the support of the U. S. Department of Energy (DE-PS36-03GO93007) for this project.

Literature Cited

1. Lai Z, Bonilla G, Diaz I, Nery JG, Sujaoti K, Amat MA, Kokkoli E, Terasaki O, Thompson RW, Tsapatsis M, Vlachos DG. Microstructural optimization of a zeolite membrane for organic vapor separation. *Science*. 2003;300:456–460.
2. Masuda T, Fukumoto N, Kitamura M, Mukai SR, Hashimoto K, Tanaka T, Funabiki T. Modification of pore size of MFI-type zeolite by catalytic cracking of silane and application to preparation of H_2-separating zeolite membrane. *Microporous Mesoporous Mater*. 2001;48:239–245.
3. Flanders CL, Tuan VA, Noble RD, Falconer JL. Separation of C6 isomers by vapor permeation and pervaporation through ZSM-5 membranes. *J Membr Sci*. 2000;176:43–53.
4. Smitha B, Suhanya D, Sridhar S, Ramakrishna M. Separation of organic-organic mixtures by pervaporation—a review. *J Membr Sci*. 2004;241:1–21.
5. Feng X, Huang RYM. Liquid separation by membrane pervaporation: a review. *Ind Eng Chem Res*. 1997;36:1048–1066.
6. Nair S, Lai Z, Nikolakis V, Xomeritakis G, Bonilla G, Tsapatsis M. Separation of close-boiling hydrocarbon mixtures by MFI and FAU membranes made by secondary growth. *Microporous Mesoporous Mater*. 2001;48:219–228.
7. Bakker WJW, Kapteijn F, Poppe J, Moulijn JA. Permeation characteristics of a metal-supported silicalite-1 zeolite membrane. *J Membr Sci*. 1996;117:57–78.
8. Kapteijn F, Bakker WJW, van de Graaf J, Zheng G, Poppe J, Moulijn JA. Permeation and separation behaviour of a silicalite-1 membrane. *Catal Today*. 1995;25:213–218.
9. Zhu X, Wang H, Lin YS. Effect of the membrane quality on gas permeation and chemical vapor deposition modification of MFI-type zeolite membranes. *Ind Eng Chem Res*. 2010;49:10026–10033.
10. Bernal MP, Coronas J, Menendez M, Santamaria J. Separation of CO_2/N_2 mixtures using MFI-type zeolite membranes. *AIChE J*. 2004;50:127–135.
11. Liu Q, Noble RD, Falconer JL, Funke HH. Organics/water separation by pervaporation with a zeolite membrane. *J Membr Sci*. 1996;117:163–174.
12. Tuan VA, Li S, Falconer JL, Noble RD. Separating organics from water by pervaporation with isomorphously-substituted MFI zeolite membranes. *J Membr Sci*. 2002;196:111–123.
13. Kuhn J, Gross J, Kapteijn F. Tuning the framework polarity in MFI membranes by deboronation: effect on mass transport. *Microporous Mesoporous Mater*. 2009;125:39–45.
14. Sano T, Yanagishita H, Kiyozumi Y, Mizukami F, Haraya K. Separation of ethanol/water mixture by silicalite membrane on pervaporation. *J Membr Sci*. 1994;95:221–228.
15. Noack M, Kolsch P, Caro J, Schneider M, Toussaint P, Sieber I. MFI membranes of different Si/Al ratios for pervaporation and steam permeation. *Microporous Mesoporous Mater*. 2000;35–36:253–265.
16. Zhu W, Gora L, van den Berg AWC, Kapteijn F, Jansen JC, Moulijn JA. Water vapour separation from permanent gases by a zeolite-4A membrane. *J Membr Sci*. 2005;253:57–66.
17. Tang Z, Kim SJ, Reddy GK, Dong J, Smirniotis P. Modified zeolite membrane reactor for high temperature water gas shift reaction. *J Membr Sci*. 2010;354:114–122.
18. Kanezashi M, O'Brien J, Lin YS. Thermal stability improvement of MFI-type zeolite membranes with doped zirconia intermediate layer. *Microporous Mesoporous Mater*. 2007;103:302–308.
19. Pan M, Lin YS. Template-free secondary growth synthesis of MFI type zeolite membranes. *Microporous Mesoporous Mater*. 2001;43:319–327.
20. Kanezashi M, O'Brien J, Lin YS. Template-free synthesis of MFI-type zeolite membranes: permeation characteristics and thermal stability improvement of membrane structure. *J Membr Sci*. 2006;286:213–222.
21. Xomeritakis G, Gouzinis A, Nair S, Okubo T, He M, Overney RM, Tsapatsis M. Growth, microstructure, and permeation properties of supported zeolite (MFI) films and membranes prepared by secondary growth. *Chem Eng Sci*. 1999;54:3521–3531.
22. Tsuru T, Igi R, Kanezashi M, Yoshioka T, Fujisaki S, Iwamoto Y. Permeation properties of hydrogen and water vapor through porous silica membranes at high temperatures. *AIChE J*. 2011;57:618–629.
23. O'Brien-Abraham J, Kanezashi M, Lin YS. A comparative study on permeation and mechanical properties of random and oriented MFI-type zeolite membranes. *Microporous Mesoporous Mater*. 2007;105:140–148.
24. Xomeritakis G, Nair S, Tsapatsis M. Transport properties of alumina-supported MFI membranes made by secondary (seeded) growth. *Microporous Mesoporous Mater*. 2000;38:61–73.
25. Uguina MA, de Lucas A, Ruiz F, Serrano DP. Synthesis of ZSM-5 from ethanol-containing systems. Influence of the gel composition. *Ind Eng Chem Res*. 1995;34:451–456.
26. Kanezashi M, Lin YS. Gas permeation and diffusion characteristics of MFI-type zeolite membranes at high temperatures. *J Phys Chem C*. 2009;113:3767–3774.
27. Matsukata M, Nara T, Kikuchi E, Miachon S, Dalmon JA. Effect of water adsorption on MFI-type zeolite membrane prepared by in situ hydrothermal crystallization. *Fuel Chem Div Prepr*. 2003;48:487–488.
28. Yang M, Crittenden BD, Perera SP, Moueddeb H, Dalmon JA. The hindering effect of adsorbed components on the permeation of a non-adsorbing component through a microporous silicalite membrane: the potential barrier theory. *J Membr Sci*. 1999;156:1–9.

29. Vroon ZAEP, Keizer K, Gilde MJ, Verweij H, Burggraaf AJ. Transport properties of alkanes through ceramic thin zeolite MFI membranes. *J Membr Sci*. 1996;113:293–300.
30. Bolis V, Busco C. Thermodynamic study of water adsorption in high-silica zeolites. *J Phys Chem B*. 2006;110:14849–14859.
31. Trzpit M, Soulard M, Patarin J, Desbiens N, Cailliez F, Boutin A, Demachy I, Fuchs AH. The effect of local defects on water adsorption in silicalite-1 zeolite: a joint experimental and molecular simulation study. *Langmuir*. 2007;23:10131–10139.
32. Bordiga S, Roggero I, Ugliengo P, Zecchina A, Bolis V, Artioli G, Buzzoni R, Marra GL, Rivetti F, Spano G, Lamberti C. Characterisation of defective silicalites. *J Chem Soc Dalton Trans*. 2000;3921–3929.
33. Fickel DW, Shough AM, Doren DJ, Lobo RF. High-temperature dehydrogenation of defective silicalites. *Microporous Mesoporous Mater*. 2010;129:156–163.
34. Coudert FX, Cailliez F, Vuilleumier R, Fuchs AH, Boutin A. Water nanodroplets confined in zeolite pores. *Faraday Discuss*. 2009;141:377–398.

Manuscript received Jan. 3, 2011, and revision received Mar. 5, 2011.